

Supplementary Information

Additive engineering by RbCl for efficient carbon based perovskite solar cells

Jun Zhang^{1,2,#}, Nian Cheng^{3,#}, Peng-an Zong^{1,2,*}, Fawang He², Jiawei Zhao², Ni Luo², Chunchang

Chen¹, Zhenguo Liu^{2,4}, Wei Huang^{2,4}

¹ College of Materials Science and Engineering, Nanjing Tech University, Nanjing 211800, China

² Key laboratory of Flexible Electronics of Zhejiang Province, Ningbo Institute of Northwestern Polytechnical University, Ningbo 315103, China

³ School of Physics and Optoelectronic Engineering, Yangtze University, Jingzhou, 434023 China

⁴ Frontiers Science Center for Flexible Electronics, Institute of Flexible Electronics, Northwestern Polytechnical University, Xi'an 710072, China

[#] These authors contribute equally to this work.

* Corresponding authors: georgepazong@gmail.com (Dr. Peng-an Zong)

Experimental Section

Materials:

Colloidal tin oxide nanoparticles (SnO_2 , 15%) were procured from Alfa Aesar. High-purity chemical reagents, including N,N-dimethylformamide (DMF, 99.9%), dimethyl sulfoxide (DMSO, 99.9%), Chlorobenzene (CB, 99.9%), and isopropanol (IPA, 99.5%), were sourced from Sigma-Aldrich. High-grade lead iodide (PbI_2 , 99.99%) was obtained from TCI, while methylammonium iodide (MAI, 99.5%) and formamidinium iodide (FAI, 99.5%) were procured from Xi'an Yuri Solar Co., Ltd. Rubidium Chloride (RbCl , 99.8%) was acquired from Sigma, and reliable carbon paste was sourced from Shanghai Materwin New Materials Co., Ltd.

Preparation of carbon pastes:

As illustrated in **Figure 1b**, the process for treating the carbon paste is presented. To mitigate the risk of harm or interference from the commercial carbon paste on the perovskite films, we subjected the commercial carbon paste to a thorough evaporation at 100°C for 48 hours, effectively eliminating any organic solvents that might negatively affect the perovskite film. Subsequently, 4.5 grams of the dried carbon particles were placed in a ball milling container and mixed with 10 mL of CB. After 12 hours of ball milling, we obtained a low-temperature carbon paste suitable for immediate use.

Device fabrication:

All devices were meticulously fabricated on etched ITO conductive glass substrates. The ITO glass substrates underwent a thorough cleaning regimen, commencing with ultrasonication in a sequential process involving anhydrous ethanol, detergent, ultrapure water, isopropanol, and anhydrous ethanol, each for a duration of 15 minutes. Subsequently, they underwent an additional cleaning step, lasting 15 minutes, utilizing an ultraviolet ozone cleaner (UVO) prior to deployment. The SnO₂ colloidal solution was judiciously diluted to a concentration of 5 wt% and applied via spin-coating onto the ITO glass substrates. This process was carried out at 4000 rpm for 20 seconds, and the coated substrates were subsequently subjected to annealing at 150 °C for a duration of 30 minutes. The perovskite precursor solution was meticulously prepared by dissolving 691.5 mg of PbI₂, 214.6 mg of MAI, and 25.8 mg of FAI in a 1 mL mixed solution of DMSO and DMF, wherein the volume ratio of V_{DMSO} to V_{DMF} was maintained at 1:9. This solution was stirred continuously for a period of 6 hours. Then, add the corresponding concentration of RbCl to the solution and continue stirring for 2 hours. Subsequently, the precursor solution was spin-coated atop the SnO₂ layer at 4000 rpm for 30 seconds, with the timely addition of 180 μL of chlorobenzene (CB) as an anti-solvent within 6-7 seconds. This was followed by a meticulous annealing process at 120 °C for a duration of 10 minutes. Finally, a layer of carbon paste was expertly blade-coated directly onto the surface of the perovskite film and subsequently annealed at 100 °C for 10 minutes.

Characterizations:

The samples underwent X-ray diffraction (XRD) analysis utilizing a Cu K α radiation X-ray diffractometer (Rigaku, Ultima IV). Surface morphology analysis was carried out using Focused Ion Beam Scanning Electron Microscope (TESCAN, S9000X Xe Plasma FIB-SEM). Infrared (IR) spectroscopy was performed with a Fourier-transform infrared spectrometer (Bruker, INVENIO-S). Surface X-ray photoelectron spectroscopy spectra of the thin film samples were acquired utilizing an X-ray photoelectron spectrometer (Thermo Science, K-Alpha). The thin film's UV-Visible absorption spectra were meticulously measured using a UV-Visible spectrophotometer (Shimadzu, UV-1800). Use ultraviolet photoelectron spectroscopy (Thermo Science, Escalab Xi+) to analyze the maximum value of the valence band in the film. Photoluminescence spectra and carrier lifetimes of the samples were obtained employing a time-resolved photoluminescence spectrometer (Edinburgh Instruments, FLS1000). Under dark conditions, the electrochemical impedance spectrum was measured using an electrochemical workstation(CH Instruments, CHI660E) at a bias voltage of 0.7 V applied to the device. Current-voltage (J-V) measurements were meticulously carried out with a Keithley 2461 source meter and a solar simulator (Enlitech, SS-X160R) under simulated AM 1.5G solar illumination (100 mW cm⁻²).

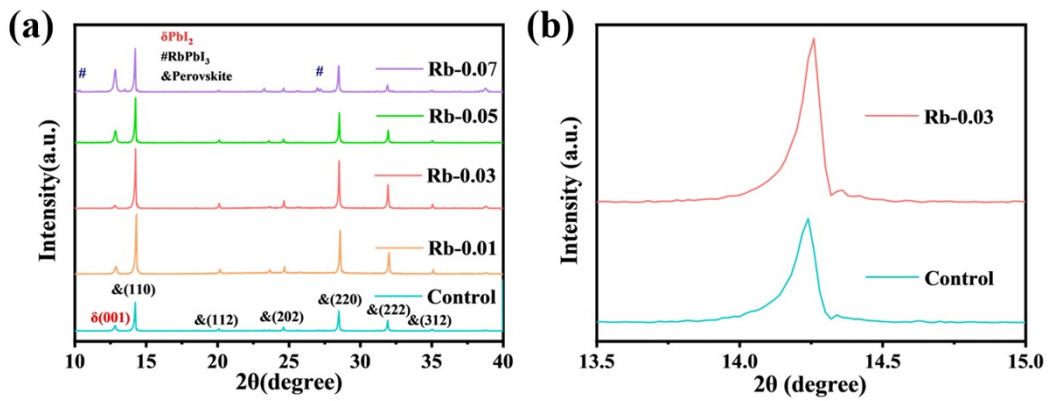


Fig. S1. (a) XRD patterns of the Control, Rb-0.03 and Rb-0.05 films; (b) local magnification of the (110) region of the Control and Rb-0.03 films.

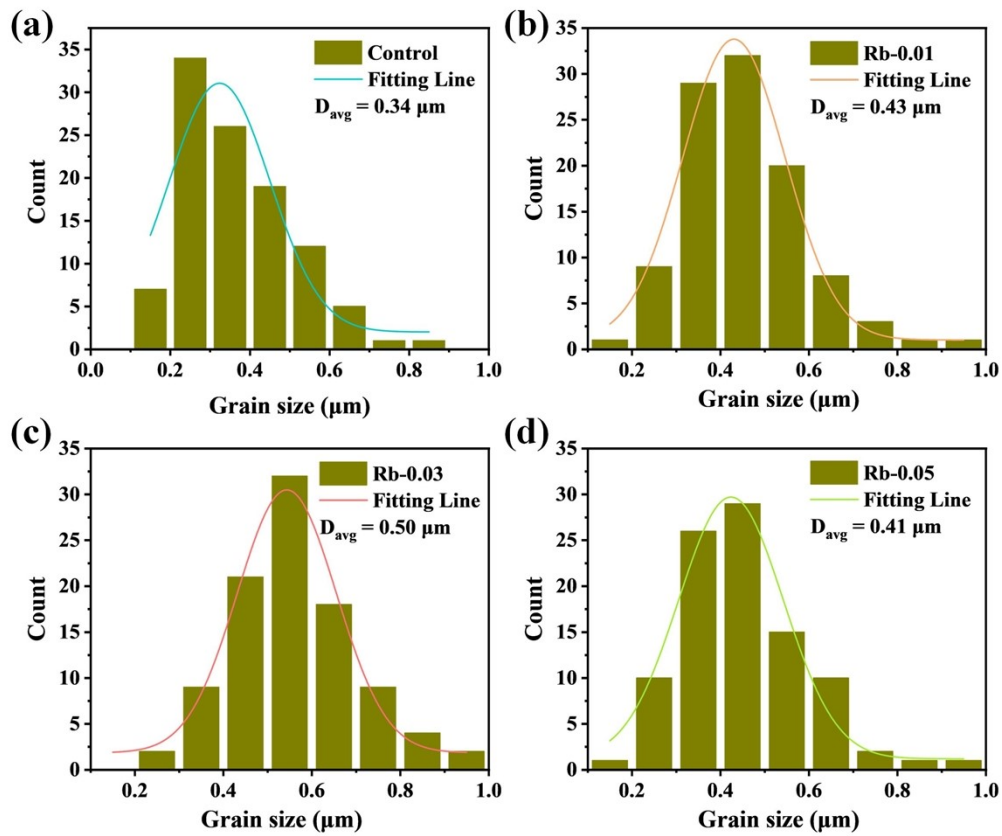


Fig. S2. Crystal size distribution diagram of (a) Control; (b) Rb-0.01; (c) Rb-0.03; (d) Rb-0.05 films.

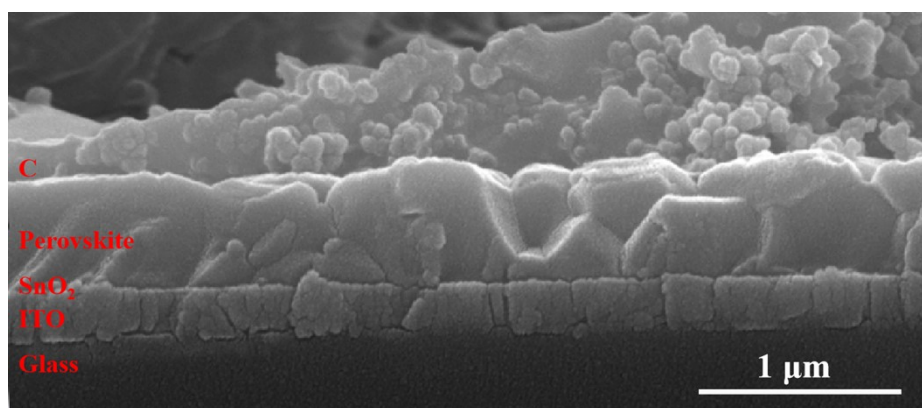


Fig. S3. Cross-sectional SEM of Rb-0.03 C-PSC device.

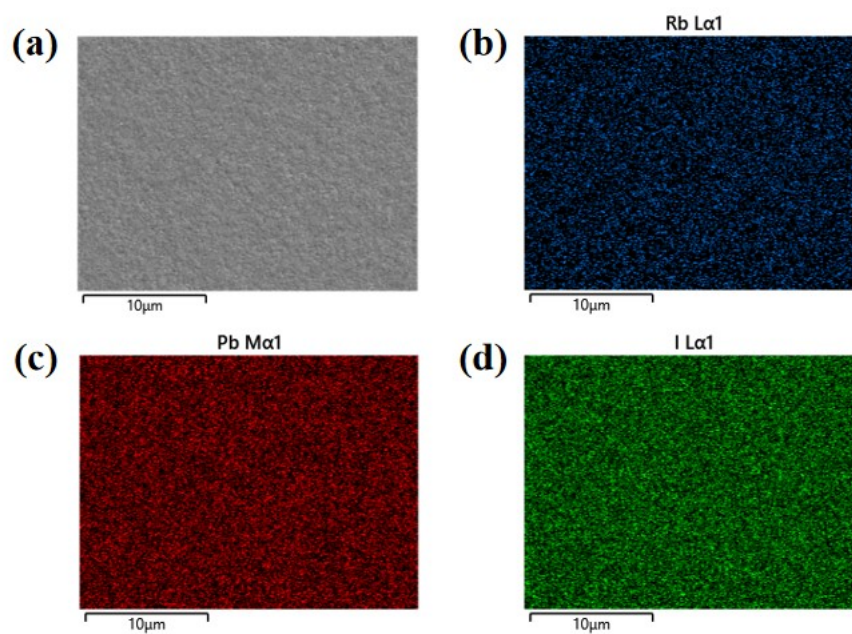


Fig. S4. EDS images of Rb-0.03: (a) SEM image; (b) Rb ; (c) Pb; (d) I element distribution.

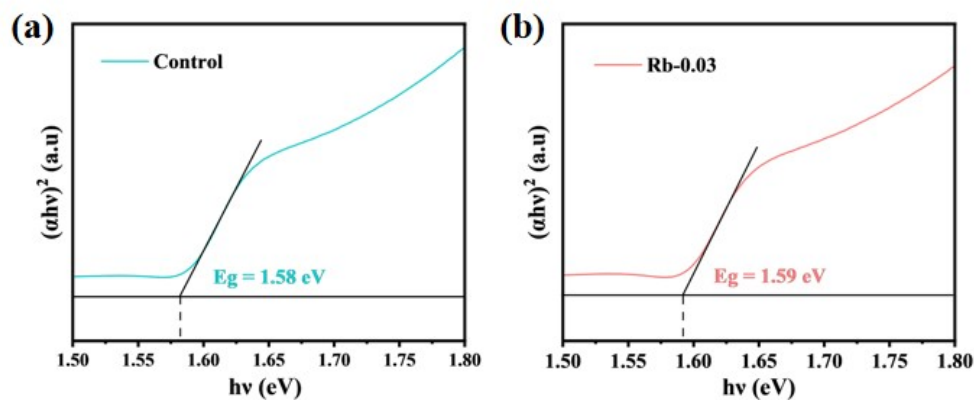


Fig. S5. Tauc plots of the Control (a) and Rb-0.03 (b) perovskite films.

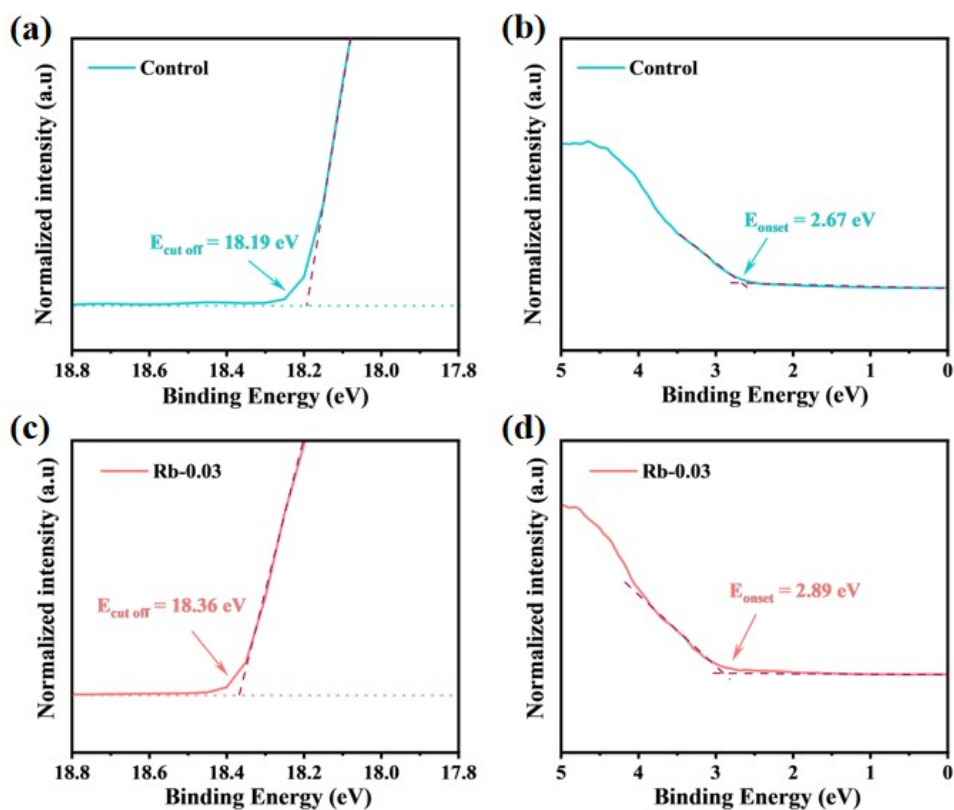


Fig. S6. E_{cutoff} of the Control (a) and Rb-0.03 (c) perovskite films; E_{onset} of the Control (b) and Rb-0.03 (d) perovskite films.

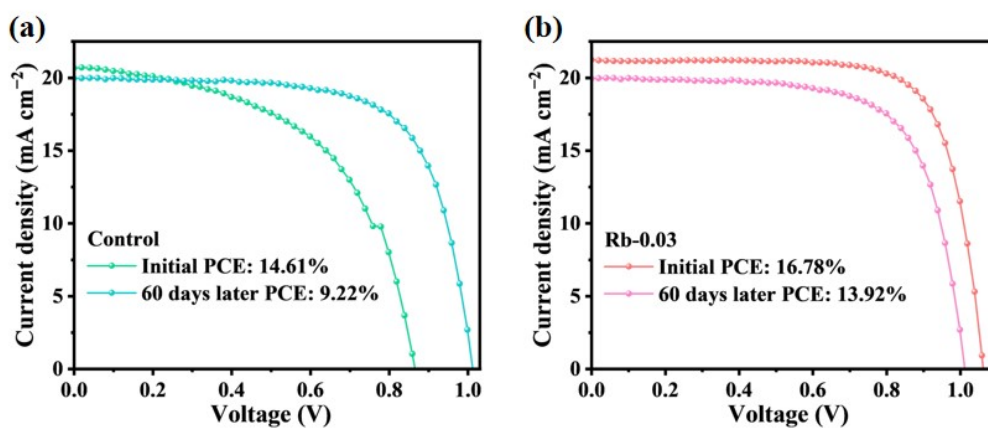


Fig. S7. Comparison of J-V curves between initial and after 60 days: (a) Control device; (b) Rb-0.03 device.

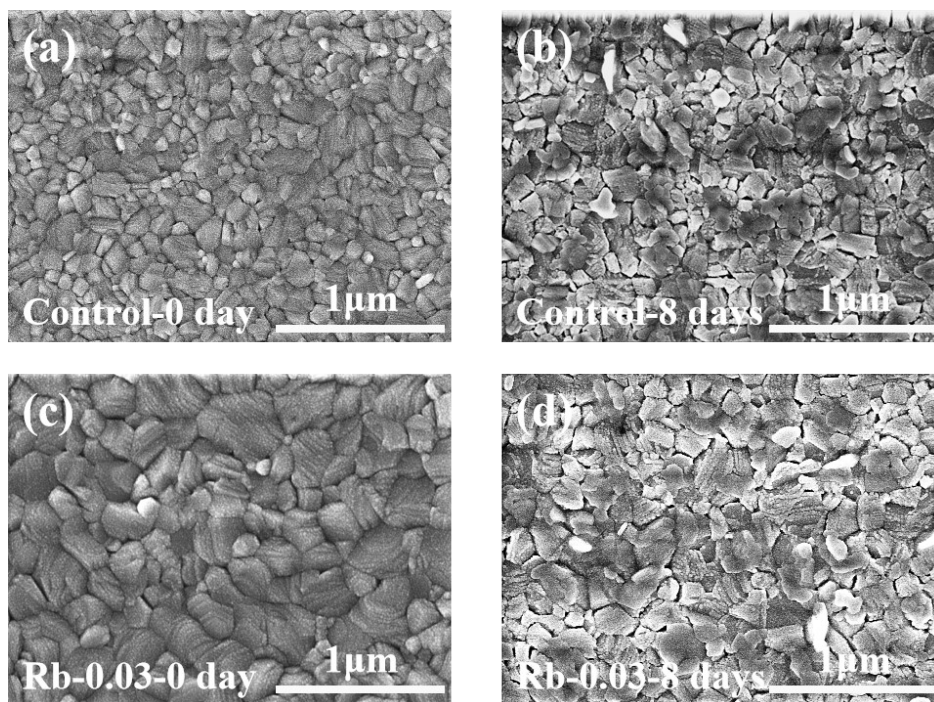


Fig. S8. SEM images of the Control (a,b) and Rb-0.03 (c,d) films before and after 8 days.

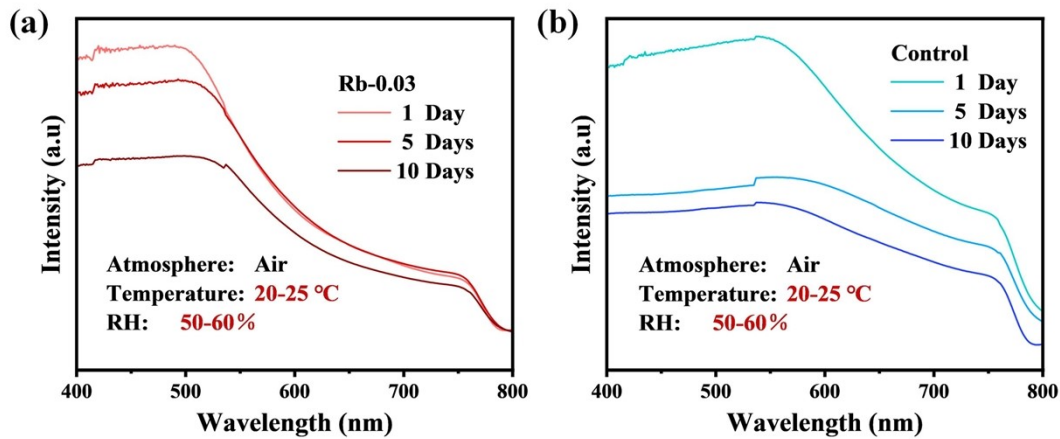


Fig. S9. UV-visible absorption spectra of the perovskite films after aging for different durations: (a) Control; (b) Rb-0.03 films.

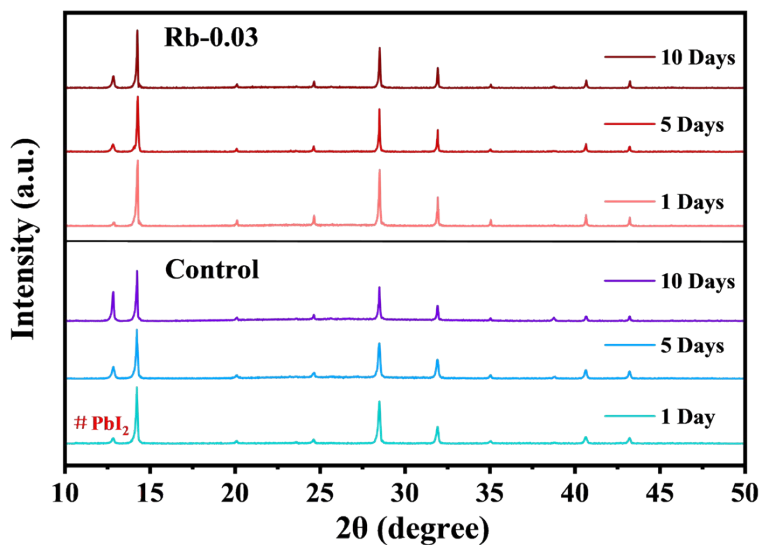


Fig. S10. XRD of perovskite films aged in ambient air for different durations for the Control and the Rb-0.03 sample.

Table S1. Reffective and teffective of Control and perovskite films doped with different concentrations of RbCl

Devices	Control	Rb-0.01	Rb-0.03	Rb-0.05
$r_{\text{effective}} (\text{\AA})$	2.206	2.199	2.185	2.172
$t_{\text{effective}}$	0.919	0.917	0.914	0.912

Table S2. TRPL Fitting Values for Control and Rb-0.03 Perovskite Films

Devices	A_1	τ_1 (ns)	A_2	τ_2 (ns)	T_{avg} (ns)
Control	0.9958	21.48	0.0358	178.96	57.81
Rb-0.03	0.7853	52.68	0.2451	203.07	134.79

Table S3. Photovoltaic parameters and hysteresis index of Control and Rb-0.03 devices during forward and reverse scanning

Devices	V_{OC} (V)	J_{SC} (mA cm^{-2})	FF (%)	PCE (%)	HF (%)
Control-RS	0.999	20.90	70.24	14.61	7.39
Control-FS	0.998	19.98	68.19	13.53	
Rb-0.03-RS	1.045	21.49	75.02	16.85	4.51
Rb-0.03-FS	1.027	21.22	73.48	16.08	

Table S4. Nyquist plot fitting data for Control and Rb-0.03 Devices

Devices	R_s (Ω)	R_{rec} (Ω)
Control	26.98	4267
Rb-0.03	23.69	7929